Infrared Spectroscopic Study of the Effect of Electrostatic Interaction on the Molecular Arrangement in the Hydration Shell around Li^+ in a Nafion Membrane

Reikichi Iwamoto*,† and Masahiro Sato‡

NIRS Institute of Water, Yuyamadai 2-7-10, Kawanishi, Hyogo 666-0137, Japan, and KRI, Incorporated, Chudojiminami-machi 134, Shimogyo-ku, Kyoto 600-8013, Japan

Received: July 22, 2009; Revised Manuscript Received: October 7, 2009

In the present paper we characterize the hydration shell around a Li ion, as $-SO_3^-Li^+$, from a series of infrared spectra of the hydrated Li salt in a sample of Nafion. The infrared spectrum significantly changes through prolonged dehydration under a controlled flow of drying gas, to a limiting dryness level. We found that the Nafion membrane contains a small population of the $SO_3^-Li^+$ group *isolated* in a hydrophobic matrix (denoted A) in addition to the main component of the *clustered* group (B). The second hydration shell around A evaporates at moderate levels of dehydration, followed by partial evaporation of the first hydration shell during the final stage. In contrast, in the hydration shell around B, which occupies a hydrophilic environment, the innermost layer of the second shell still remains unevaporated under full dehydration conditions. From the hydration shell around A, we were able to resolve the distinct fundamental bands ν_3, ν_1, and ν_2 of the water that is coordinated to Li^+ in the first hydration shell. From analysis of the infrared spectrum of the hydration shell around B, we found that the strong electrostatic field of Li^+ brings about a molecular arrangement that is *less favorable* for intermolecular hydrogen-bonding in the *inner* second hydration shell. This structural effect occurs to a minor extent for the second hydration shell around a Na ion, which has a significantly weaker electrostatic field.

Introduction

Elucidation of the molecular arrangement and structure in the hydration shell around a metal ion is a basic and important step toward understanding various properties of metal ions in aqueous solution. As the smallest alkali metal ion, and possessing high water solubility, lithium is an appropriate ion to use in studies on the effects of a strong electrostatic field on the water in its close vicinity.

Many experimental and theoretical studies have been made of the hydration shell of a Li ion.[1−28] The hydration shell around Li^+ has been studied by X-ray and neutron diffraction methods.[1−7] It was reported that water molecules in the first hydration shell are coordinated to Li^+, having a definite O−Li distance of 1.95 Å and a coordination number of 3.3−5.5.[4,7] Some diffraction studies reported the existence of a second hydration shell outside the first.[5,7]

Recently, increasing numbers of theoretical studies on the hydration shell of Li^+ have been reported. Babu and Lim reported a study of the hydration shell of alkali and alkaline earth metal ions by means of molecular dynamics simulations.[12] By extending the number of hydrating water molecules to eight, Hashimoto and Kamimoto theoretically predicted that Li^+ interacts electrostatically not only with the first hydration shell but also with the second hydration shell to a considerable extent.[10] Miller and Lisy reported infrared photodissociation spectra and ab initio calculations of interaction energies and structures for $M^+(H_2O)_n$ ($n = 1-6$) hydration clusters of alkali metal ions.[24,25] Watanabe and Ooi theoretically studied stable structures of the hydration shell around the Li^+ in SO_3Li and COOLi as models for the hydrated state of a perfluorinated Nafion Li salt membrane.[21] Petit et al. theoretically studied the dynamics of the hydration around Li^+ in highly concentrated LiCl aqueous solution.[27] They predicted that hydration clusters with three different compositions of H_2O and Cl occur. Many authors reported from theoretical calculations that the hydration energy of the first hydration shell is significantly larger for Li^+ ion than for other alkali metal ions, although the hydration energy is even larger for divalent ions such as the Be ion.[10,12,17,19,22,26] The coordination number of 4 was reported for the water in the first hydration shell around Li^+ by a combined ab initio quantum mechanical and molecular mechanical-molecular dynamics simulation method,[9,10,12,14,19,20,22,24] in agreement with experimental results.[4,7] Normal vibrations were also calculated for the hydrating water molecules,[8,13,14] although reliable spectral data, which could be compared with the calculated frequencies, were not always available.

On the other hand, infrared and Raman spectra give important structural information on the hydration shell of Li^+, since the OH stretching frequencies and the band shape of the infrared or Raman bands are sensitive to the interactions of the water.[29−31] In aqueous solution of an ion, however, the bulk water and even the water just outside the hydration shell has a predominant contribution to the infrared absorption or Raman scattering, so that it is extremely difficult to separate a *very small contribution* of the hydrating water in the close vicinity of an ion from the much larger contribution of the bulk and the outer hydration sphere. However, if the interaction brings about a new band at a sufficiently resolved position from that of the bulk, it is possible to observe a reliable signal of the hydration shell. In fact, a low-frequency Raman peak, which was assigned to the Li−O stretching vibration, was observed even at low concentrations.[32] An attempt was made to resolve the infrared spectra of "pure salt-solvated" water in aqueous solutions of

* Corresponding author. Phone: (81)72-792-4998. Fax: (81)72-792-4998. E-mail: iwamoto@kjb.biglobe.ne.jp.
† NIRS Institute of Water.
‡ KRI, Incorporated.

10.1021/jp906934u CCC: $40.75
Published on Web 10/30/2009

various alkali halide salts.[33] FT-IR spectroscopy utilizing isotope dilution was applied to separate the absorptions due to the hydration shell around Li, Na and K ions in aqueous solution.[34] Dielectric spectroscopy was applied to study the association and hydration in aqueous solutions of Li salts, and the analysis indicated that Li^+ has a significant second solvation sheath.[35] Recently, new infrared and Raman spectroscopic methods were developed to study the structure or dynamics of water in the close vicinity of an ion in aqueous solution.[36−38]

In the present paper, we studied the infrared spectra of the water contained in the perfluorinated alkali metal salt ionomer or Nafion membrane, which has the chemical structure[39] where

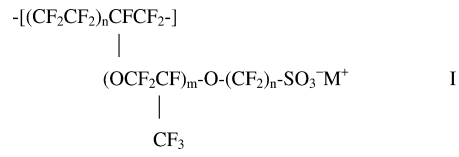

I

$m = 0-1$ and $n = 1-5$. The membrane polymer, which consists of a hydrophobic fluorocarbon main chain and a short fluorocarbon oxide branch with a terminal *hydrophilic* sulfonate group, has a two-phase structure, in which the *hydrophilic* ionic clusters of microscopic dimension are dispersed in the *hydrophobic* fluorocarbon matrix.[39−45] The ionic clusters absorb "a maximum of 15−30% water by weight, which corresponds to about 10−20 water molecules per ionic group",[39] and most of the absorbed water is gathered at the *hydrophilic* ionic clusters.[40,41] The water, which is collected in the *hydrophilic* portion of ionic clusters, may be taken as "an enclosed microscopic drop" of highly concentrated aqueous solution of $SO_3^-M^+$ and contains little "bulk" water, which often seriously interferes with infrared spectroscopic observation of the water in close vicinity to the ion. In addition, the "solution" may be further concentrated by pervasive evaporation through the membrane matrix, and only a small number of water molecules may remain around a $SO_3^-Li^+$ group at the limiting dehydration. This makes it possible for us to investigate the infrared spectrum of the hydration shell, which changes during the whole dehydration process. Thus, the Nafion membrane is an ideal material by which we can selectively study the hydration shell around a metal ion without disturbance of bulk water.

Falk et al. reported infrared spectra of the water contained in the membrane of the Nafion salts of various ions of alkali, alkali-earth and other metals.[46,47] They interpreted the multiple OH stretching bands observed of the water in terms of two different proton environments in the membrane.[47] In our previous study,[48] from analysis of the changing infrared spectrum during dehydration, we found that water contained in the Nafion membrane mostly exists as hydronium ions.[48] In the present study we followed the infrared spectrum of the hydrated Nafion alkali metal salt membrane through the whole drying process to its limiting dehydration level. In the course of the study, we found that the membrane has a small population of the SO_3Li groups, which are isolated in a hydrophobic matrix, in addition to the main clustered groups, which are hydrophilic. Analysis of the infrared spectra of the hydrated Nafion salt membrane during prolonged dehydration has given us a picture of the "whole" hydration shell around Li^+.

Experimental Section

Sulfonic acid-type Nafion membranes of 30 μm thickness were obtained courtesy of Asahi Glass Co., Ltd. The sample was treated in a 1% solution of alkali metal hydroxide at room temperature to give the alkali metal salt. After treatment, the membrane was thoroughly washed with distilled water to remove contaminating alkali metal hydroxide. The treated membrane, denoted as $RSO_3^-M^+$ (M^+: alkali metal ions), where R stands for the fluorocarbon component other than the $SO_3^-M^+$ group of the chemical structure of I, was used in the present paper.

The instrument used was a Nicolet Magna 760 Fourier transform infrared (FT-IR) spectrometer, equipped with a KBr/Ge beam splitter and a DTGS detector. The spectrum of a membrane was measured with a resolution of 4 cm^{-1} and 100 scans mostly in a drying cell, described below, and sometimes without the cell, in the spectrometer under purging with dry air at room temperature.

The Li (or other alkali metal ion) salt membrane, fully hydrated to atmospheric humidity, was the starting sample for the spectral measurements. The sample was set in a specially designed drying cell with CaF_2 windows, possessing a volume of 20 mL, through which drying N_2 gas was let flow at a controlled rate from 10 to 500 mL/min. The spectrum of a sample was continuously measured through the whole drying process to its limiting dehydration level.

It was not possible to quantitatively measure the weight of the water contained in a sample, not only because the sample too quickly absorbs moisture in air in the outside but also because the moisture contained in a sample is too small to be weighed. The peak-height or area intensity of a band was measured by the use of the built-in programs in the spectrometer with an appropriate baseline, which connects two points appropriately selected at both sides of a peak in question.

Results and Discussion

Infrared Spectral Changes of Hydrated Alkali Metal Salt Nafion Membranes during Dehydration. Figure 1 shows a series of infrared spectra of a hydrated $RSO_3^-Li^+$ membrane, which changes through the dehydration process to the limiting dryness level. Spectrum a is of the initial sample that was fully hydrated to atmospheric humidity. The other spectra are of the same sample being dehydrated under various flow rates of drying N_2 gas, as shown in Table 1. Spectrum h is of the sample that was most completely dried by the dehydration method. In spectrum a, the strong band at 3517 cm^{-1} is assigned to the OH stretching band (the notation ν(OH) is used, hereafter, to indicate a nonsplit OH stretching band of water) of the water in the hydration shell. The band at 1635 cm^{-1} is assigned to the OH deformation band (the notation δ(OH), instead of ν_2, is used, hereafter, to denote the OH deformation band of the water with a nonsplit OH stretching band). The weak bands around 2900, 2350, and 1700 cm^{-1} are assigned to the membrane polymer.[49] As dehydration of the membrane proceeds, the ν(OH) and δ(OH) bands of the water decrease in intensity and shift in mutually opposite directions. In addition, when dehydrated to some extent, two weak shoulders appear on the high-frequency slope of the ν(OH) band as in the spectrum c. When further dehydrated, the shoulders become clearer to show two distinct peaks at 3703 and 3640 cm^{-1}, and the δ(OH) band shifts downward finally to 1628 cm^{-1} with an obscured shoulder near 1615 cm^{-1}, as in the spectrum h.

To analyze the observed spectral changes following dehydration in relation to the influence of a Li ion, we characterized the binding properties of the hydration shell. We used "the duration of drying gas flow at a flow rate" before a measurement as an index of the property. Table 1 gives the flow rate and its

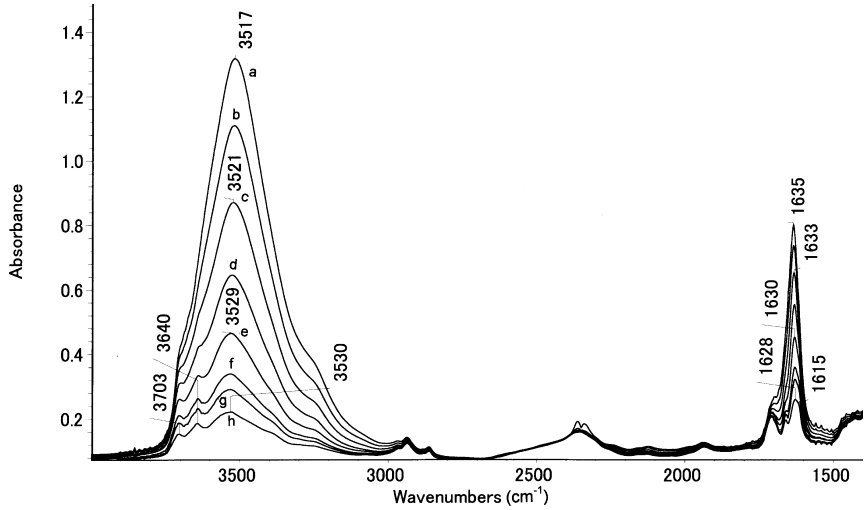

Figure 1. Series of infrared spectra of a hydrated Nafion salt membrane $RSO_3^-Li^+$ during prolonged dehydration to its limiting dryness level, the drying proceeding in sequence from a to h as in Table 1.

TABLE 1: Measurement Conditions for a Series of Spectra, Shown in Figure *1*, of an Initially Fully Hydrated Sample of the $RSO_3^-Li^+$ Membrane during the Whole Dehydration Process to Its Limiting Dryness Level

	measurement number								
	0	1	2	3	4	5	6	7	8
spectrum	a	b	c	d	e		f	g	h
flow rate (mL/min)	0	20	20	20	50	500	500	500	500
meas time (min)[a]		6	16	48	51	79	273	620	2439
$A/A(0)$[b]	1.0	0.83	0.64	0.46	0.32	0.27	0.22	0.18	0.12
$A(Q)/A$[c]					0.043	0.048	0.057	0.060	0.066

[a] Time duration in minutes after a flow rate was newly set. [b] $A/A(0)$ is the ratio of the area intensity (A) of the band at about 3520 cm^{-1} in a spectrum to that in the spectrum a ($A(0)$). [c] $A(Q)/A$ is the ratio of a combined area intensity $A(Q)$ of the two bands at about 3700 and 3640 cm^{-1} to A.

duration before each measurement, together with some spectral quantities in the measured spectra. The top line gives a sequential number of measurements, and "0" denotes the initial state. The notations of a, b, etc. in the first line correspond to those of the spectra in Figure 1. The second line gives the flow rate of drying gas at the time of a measurement. The third line gives a time passage at a measurement after a new flow rate was set. The fourth line gives the ratio of an area intensity A of the band around 3520 cm^{-1} over the 3700−3000 cm^{-1} range in a spectrum to the intensity in the spectrum a or $A(0)$. The ratio $A/A(0)$ gives the fraction of the hydration shell that remains in the membrane at the time of a measurement. The bottom line gives the ratio of the combined area intensity ($A(Q)$) of the bands at 3703 and 3640 cm^{-1} with a common baseline between the positions of about 3750 and 3600 cm^{-1} to the area intensity A of the band around 3520 cm^{-1}.

As shown in Table 1, about half of the water contained evaporates within 48 min at a slow flow rate of 20 mL/min. When the flow rate was increased to 50 mL/min, the remaining fraction decreased to about one-third in about 50 min. After this, the evaporation rate of the hydration shell becomes much slower. The ratio $A/A(0)$ decreases from 0.32 to 0.22 in 273 min at the high flow rate of 500 mL/min. Additional prolonged dehydration for about 2000 min causes a small decrease in $A/A(0)$ from 0.22 to 0.12. The fraction of 0.12 of the initial content remains unevaporated even after prolonged dehydration; that is, about one tenth of the hydration shell is very strongly bound in the membrane.

The series of spectra shown in Figure 1 and the binding properties of the hydration shell given in Table 1 strongly imply that the spectrum of the hydration shell changes from the outer layer to the inner. To check this in more detail, we took differences between some pairs among the spectra in Figure 1. The difference obtained in this manner should give a spectrum of the hydration shell that evaporates during two relevant measurement times. Figure 2 shows the differences of (a − b), (e − f), and (g − h) among the spectra shown in Figure 1, where the spectrum of the latter notation in parentheses is subtracted from that of the former with a subtraction factor of 1. As is seen from Table 1, the spectrum in Figure 2x is of the outermost hydration layer, the one in Figure 2y is of an intermediate layer, and the one in Figure 2z is of the innermost layer that evaporated. The spectra in Figure 2 indicate that, as dehydration proceeds, the ν(OH) band near 3520 cm^{-1} significantly shifts upward, and the δ(OH) band at about 1630 cm^{-1} not only shifts, on the contrary, downward but also significantly increases in peak height relative to the ν(OH) band. Figure 2z shows the new well-separated weak but sharp peaks at 3704 and 3639 cm^{-1} on the high-frequency slope of the strong band at 3532 cm^{-1}. A series of the difference spectra in Figure 2, together with those in Figure 1, suggest that the hydration shell somehow changes in structure from the outer to the inner. To characterize the two bands at the high-frequency side of the main peak, we checked dependence of the intensity of the two bands relative to that of the main band (or $A(Q)/A$) on dehydration as in Table 1. The ratio gradually increases with the progress of dehydration.

Figure 3 shows a series of infrared spectra of the *hydrated* membrane sample of $RSO_3^-Na^+$. Spectrum a is that of the initial sample that was fully hydrated to atmospheric humidity, and spectrum i is of the same sample that is almost completely dehydrated. This sample shows a sharp band at 3664 cm^{-1} even

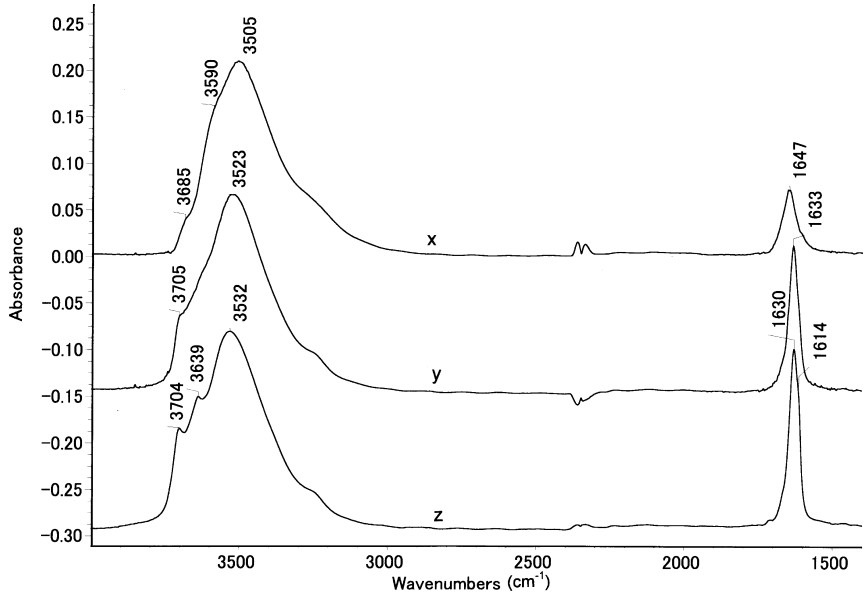

Figure 2. Difference spectra derived from spectra a−h in Figure 1. x = (a − b); y = (e − f), and z = (g − h).

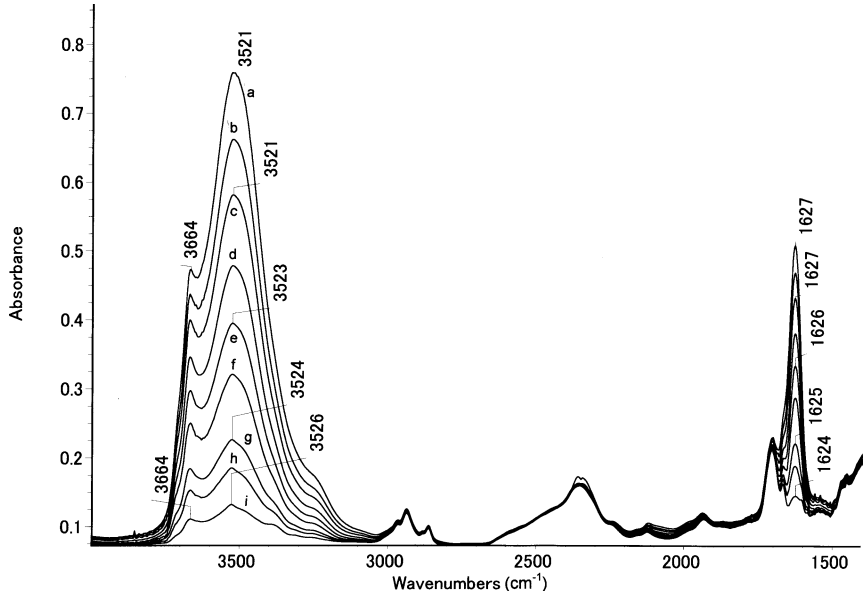

Figure 3. Series of infrared spectra of a hydrated Nafion salt membrane $RSO_3^-Na^+$ during prolonged dehydration to its limiting dryness level, the drying proceeding in sequence from a to i as in Table 2.

in the initial state, as in spectrum a, in addition to the main band at 3521 cm^{-1}. The two bands in the 3700−3300 cm^{-1} region are assigned to the ν(OH) band, and the one around 1630 cm^{-1} to the δ(OH) band, similar to the case of the Li salt membrane. The binding properties of the hydration shell in the membrane of $RSO_3^-Na^+$ are shown in Table 2, similarly to the case of $RSO_3^-Li^+$. According to $A/A(0)$ in Table 2, the hydration shell or the water content in the $RSO_3^-Na^+$ membrane decreases to about 60% for 42 min at a low flow rate of 10 mL/min, and then to about 40% for 50 min at a flow rate of 30 mL/min. As the water content decreases below this level, the evaporation rate becomes increasingly slower. The ratio $A/A(0)$ finally becomes 0.08 after the dehydration time of about 1000 min at a flow rate of 500 mL/min. Comparison of the dependence of the ratio $A/A(0)$ on the dehydration conditions in Table 2 with that in Table 1 indicates that the hydration shell in the $RSO_3^-Na^+$ membrane evaporates significantly more rapidly than that in the $RSO_3^-Li^+$ membrane. The ratio A_{3660}/A_{3520} in Table 2 indicates that the band at 3660 cm^{-1} gradually increases in intensity relative to the main band at 3520 cm^{-1} with the progress of dehydration, similar to the two bands at about 3700 and 3640 cm^{-1} in the $RSO_3^-Li^+$ membrane. This similarity suggests that the bands in the high frequency region, which commonly appear for the Li and Na salt membranes, probably have the same origin.

Here let us consider why the hydration shell shows the two ν(OH) bands of high and low frequencies. The lower-frequency band appears at nearly the same frequency of 3520 cm^{-1} for both the Na and Li salt membranes, and the higher-frequency band commonly appears in the 3705−3640 cm^{-1} region for the Li and Na membranes. The spectral characteristics of the samples, which were prepared by treating the RSO_3H Nafion membrane of the same origin, suggest that the membrane may have two different types of $SO_3^-M^+$ groups, which are hydrated in different manners. The two frequencies of about 3700 and 3640 cm^{-1} in spectrum h of the hydration shell around a $SO_3^-Li^+$ group (Figure 1 and Figure 2z) agree with those of the water that is coordinated to a Li^+ ion as in $Li^+(H_2O)_n$ (n <

TABLE 2: Measurement Conditions for a Series of Spectra, Shown in Figure 3, of an Initially Fully Hydrated Sample of the RSO_3Na Membrane during the Whole Dehydration Process to Its Limiting Dryness Level

	measurement number								
	0	1	2	3	4	5	6	7	8
spectrum	a	b	c	d	e	f	g	h	i
flow rate (mL/min)	0	10	10	10	30	30	90	500	500
meas time (min)[a]		8	17	42	14	50	132	63	1028
$A/A(0)$[b]	1.0	0.86	0.74	0.59	0.47	0.37	0.22	0.16	0.08
A_{3660}/A_{3520}	0.039	0.045	0.052	0.057	0.062	0.066	0.068	0.069	0.063

[a] Time duration in minutes after a flow rate was newly set. [b] $A/A(0)$ is the ratio of the area intensity (A) of the band at about 3520 cm^{-1} in a spectrum to that in the spectrum a ($A(0)$). [c] A_{3660}/A_{3520} is the ratio of the area intensity of the band at about 3660 cm^{-1} (A_{3660}) relative to that of the main band at around 3520 cm^{-1} (A_{3520}).

TABLE 3: Absorption Bands of the Hydration Shell in the Nafion Membranes of Li, Na, K, and Rb Salts[3]

	ν_3 (cm^{-1})	ν_H(OH) (cm^{-1})	ν_1 (cm^{-1})	ν(OH) (cm^{-1})	δ(OH) (cm^{-1})	ν_2 (cm^{-1})
Li	3703		3634	3520	1635	1615 sh
Na		3664		3521	1627	
K		3681		3526	1626	
Rb		3680		3524	1625	

[a] In the table, the ν_1, ν_2, and ν_3 modes are used for the clearly separated bands of the first hydration shell around a Li ion, ν(OH) and δ(OH) are used for the nonsplit bands, and ν_H(OH) is used to denote the high frequency band observed for Na, K, and Rb salts.

4).[24,25] The band at about 3660 cm^{-1} of the hydration shell around a $SO_3^-Na^+$ group is between the frequencies of the two bands of the water that is similarly coordinated to a Na^+ ion.[24,25] The band at 3520 cm^{-1} may be assigned to the water that is collected in ionic clusters, judging from the frequency and bandwidth. Considering this, we propose that the Nafion membrane contains a small fraction of the $SO_3^-M^+$ groups that are individually *isolated* in a hydrophobic region of the matrix, in addition to the main hydrophilic component of the *clustered* groups. In the structure, most of the water contained should gather in the *hydrophilic* clusters to form the main hydration shell, and only a small fraction of the water should gather around the group *isolated* in the *hydrophobic* matrix. Thus, the ν(OH) band at about 3520 cm^{-1} should be assigned to the hydration around $SO_3^-Li^+$, which comprises an ionic cluster, and, on the other hand, the bands in the 3705−3640 cm^{-1} region should be assigned to the hydration shell around $SO_3^-Li^+$ isolated in the hydrophobic matrix. The proposition is reasonable considering results from previous studies; that is, one water molecule is hydrogen-bonded to an isolated alcoholic OH in hydrophobic medium in a copolymer[50] of ethylene and vinyl alcohol or in a hydrophobic solution[51] of 2-nonanol in heptane, and the water contained in clustered OH groups forms combined hydrogen-bonded networks,[50,51] which show a broader absorption of a low frequency. The structure is consistent with the report by Quezado et al.[47] that one (or two) weak and sharp band appears around 3680 cm^{-1} in addition to the main band around 3520 cm^{-1} in various univalent or divalent metal salts of Nafion membranes in their highly dehydrated state.

The proposed structure for the Nafion membrane having two types of ionic groups is consistent with the observation that the hydration shell in the K and Rb salt samples of Nafion also shows two OH stretching bands, one weak band appearing around 3680 cm^{-1} and another strong band appearing around 3520 cm^{-1}, as summarized in Table 3.

We denote the clustered and isolated groups as $(SO_3^-M^+)$(Clus) and $(SO_3^-M^+)$(Isol), respectively. The hydrate of the former is expressed as

$$[SO_3^-(M^+ \cdot nH_2O) \cdot mH_2O)]\ (\mathrm{Clus}) \qquad (1)$$

where nH_2O is the first hydration shell, n being the coordination number, and mH_2O is the second hydration shell, m being the number of hydrating water molecules and variable, depending on dryness of the membrane. The hydrate of the isolated group is formulated as

$$[SO_3^-(M^+ \cdot nH_2O) \cdot sH_2O)]\ (\mathrm{Isol}) \qquad (2)$$

where nH_2O denotes the first hydration shell just as in the case of the clustered ions and sH_2O denotes the second hydration shell. The second hydration shell of sH_2O, which exists in a strongly *hydrophobic* environment, should be significantly less stable than that of mH_2O in hydrophilic environment. The number s should be much smaller than m.

Hydration Shell around a Li Ion Isolated in a Hydrophobic Matrix. Here we analyze the hydration shell of the hydrated *isolated* $SO_3^-Li^+$ group or $[SO_3^-(Li^+ \cdot nH_2O) \cdot sH_2O]$ (Isol) in (2). The second hydration shell of sH_2O, which is weakly bound in strongly hydrophobic surroundings, should evaporate at an early stage or at a middle stage during dehydration. In contrast, the first hydration shell of nH_2O, which is coordinated to a Li ion with a large hydration energy,[10,19] may resist evaporation. The evaporation process of the hydration shell of $[SO_3^-(Li^+ \cdot nH_2O) \cdot sH_2O]$ (Isol) may proceed as follows, where

$$[SO_3^-(Li^+ \cdot nH_2O) \cdot sH_2O)](\mathrm{Isol}) \rightarrow [SO_3^-(Li^+ \cdot nH_2O) \cdot tH_2O)](\mathrm{Isol}) + (s-t)H_2O(\uparrow) \rightarrow$$
$$\mathrm{P} \qquad\qquad \mathrm{Q}$$
$$\rightarrow [SO_3^-(Li^+ \cdot nH_2O)](\mathrm{Isol}) + tH_2O(\uparrow) \rightarrow [SO_3^-(Li^+ \cdot (n-x)H_2O)](\mathrm{Isol}) + xH_2O(\uparrow) \qquad (3)$$
$$\mathrm{R} \qquad\qquad \mathrm{S}$$

$H_2O(\uparrow)$ indicates evaporating water and t or x is an integer ($s \geq t \geq 0$, $n \geq x \geq 0$). Through the dehydration step of Q, the second hydration shell continues to evaporate with t decreasing, and at the step R the second shell evaporates out. At step S, the first hydration shell evaporates with x increasing.

The second hydration shell, which is weakly bound, in the evaporation scheme of (3) should have absorptions in the high frequency region in the difference spectra shown in Figure 2. The obscured shoulders in the 3700−3600 cm^{-1} region of the

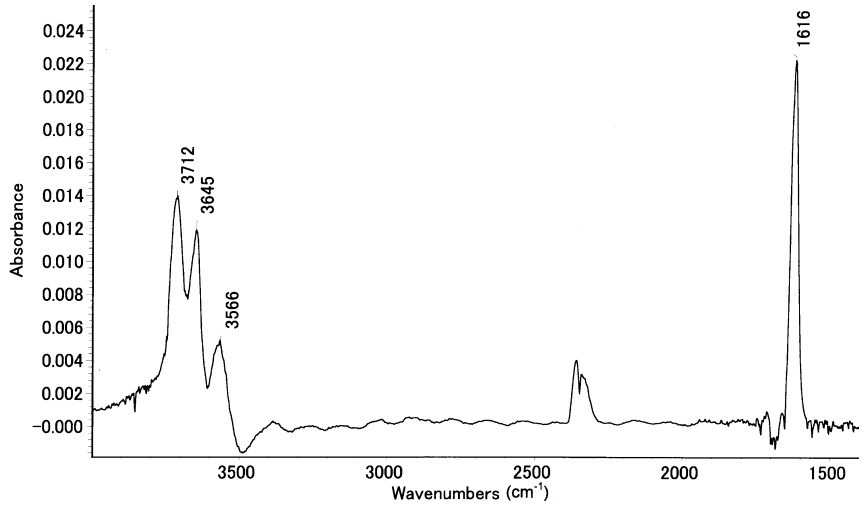

Figure 4. Separated spectrum of the first hydration shell around an isolated Li^+ ion, in which the spectrum in Figure 2y was subtracted from the spectrum in Figure 2z to cancel the band at 3532 cm^{-1}.

spectra in Figure 2x,y may be assigned to the evaporated component. These spectra and the dehydration conditions (Table 1) indicate that the second hydration shell evaporates at an early or middle stage of dehydration at the step Q. This step continues until the measurement time of the spectrum f in Figure 1 or Table 1, judging from spectrum y in Figure 2, which does not show the two clear bands. Partial evaporation of the overlaying second hydration shell makes the first hydration shell partly free from hydrogen-bonding, resulting in the appearance of the two clear bands at about 3700 and 3640 cm^{-1}, as in spectrum e in Figure 1. Before the measurement time of spectrum g, the second hydration shell completely evaporates just as in step R. After this step, the first hydration shell begins to evaporate, although the evaporation rate is very slow according to Table 1. Occurrence of step S or the evaporation of the first hydration shell is definitely verified by the appearance of the clear bands at about 3700 and 3640 cm^{-1} in the spectrum in Figure 2z.

To separate the characteristic bands of the first hydration shell from the main absorption at about 3520 cm^{-1}, we subtracted the spectrum of Figure 2y, which only just reveals the bands of the first hydration shell, from the spectrum of Figure 2z. This subtraction gives the spectrum in Figure 4, which clearly shows not only the two bands at 3712 cm^{-1} and 3645 cm^{-1} but also the distinct band at 1616 cm^{-1}. The main band around 3520 cm^{-1} is almost canceled, a weak peak remaining at 3566 cm^{-1}. The noise around 2300 cm^{-1} is due to unbalanced absorptions of CO_2 gas. The separated bands at 3712 and 3645 cm^{-1} correspond to the high-frequency bands in a series of the spectra shown in Figure 1, and the band at 1616 cm^{-1} corresponds to the shoulder in spectrum h in Figure 1, or in spectrum z in Figure 2. The separated bands at 3712 and 3645 cm^{-1} agree well in frequency with those observed for $Li^+(H_2O)_n$ ($n = 1-4$).[24,25]

The spectrum in Figure 4 shows all three fundamental bands expected of the water molecules, which are coordinated through the O atoms to a Li ion with their free H atoms outward, in the first hydration shell. The clearly separate peaks at 3712 and 3645 cm^{-1} are assigned to the ν_3 and ν_1 fundamentals, respectively, and the distinct peak at 1616 cm^{-1} is assigned to the ν_2. When an alcoholic OH is one-to-one hydrogen bonded to another OH, the frequency of the acceptor OH stretching band is minimally affected by the hydrogen bond.[51,52] The above observation indicates that the *electrostatic coordination of a* Li^+ *ion to the O atom* does not affect the frequency of the OH stretching band either. Instead, the ν_2 band in the spectrum in Figure 4 is significantly stronger than either of the ν_3 or ν_1 bands, although the opposite is usually true, as observed for the spectrum of the water molecule dissolved in poly(methyl methacrylate), for example.[53] To exemplify this distinction, we compared the intensities of the three bands relative to the ν_3 band of the water with those of the water in polyvinylidene fluoride [$(CH_2CF_2)_n$] (PVDF) in Table 4. The water, which is molecularly dissolved by weak hydrogen-bonding interactions in PVDF, shows a clear infrared spectrum.[54,55] As is seen from the table, the ν_2 band of the water in the first hydration shell around a Li ion is about twice as intense as the ν_3 band, whereas the ν_2 band of the water in PVDF is about two-thirds the intensity of the ν_3 band. We note that *the electrostatic coordination to a* Li^+ *ion does not much affect the frequencies of the* ν_1, ν_2, *and* ν_3 *vibrations of water, but it significantly influences their relative intensities*.

TABLE 4: Band Frequencies and Relative Peak Intensities of the First Hydration Shell of a Li^+ Ion and of the Water Dissolved in PVDF

matrix		ν_3	ν_1	ν_2
RSO_3Li	freq (cm^{-1})	3712	3645	1616
	rel peak intensity	1	0.82	1.93
PVDF[a]	freq (cm^{-1})	3704	3622	1616
	rel peak intensity	1	0.42	0.71

[a] Iwamoto, R. Unpublished work.

At this position we consider how the first hydration shell surrounds an isolated Li ion; the water covers the whole surface of a Li ion to separate the counterion (SO_3^-) or only partly surrounds the open space around a Li^+ ion ionically bonded to the counterion. Actually, it is not possible to determine which of the structures is true from the spectrum in Figure 4 alone, but the partly coordinated structure may be more reasonable, considering the following theoretical studies. In the stable hydration structure of $SO_3^-Li^+(H_2O)_n$ ($n = 1-5$), a Li^+ ion is coordinated not only to water but also to a SO_3^- ion.[21] The hydrates of $Li^+(H_2O)_4$, $Li^+(H_2O)_3Cl^-$, and $Li^+(H_2O)_2(Cl^-)_2$ coexist in highly concentrated solutions of LiCl.[27] This means that the coordination number n is less than four in the hydrate in (1) or (2).

In the above we have treated the first hydration shell around a Li^+ ion of the isolated $SO_3^-Li^+$ group or nH_2O in $[SO_3^-(Li^+ \cdot nH_2O) \cdot sH_2O](Isol)$. In what follows, we consider the second hydration shell or sH_2O, which should evaporate at

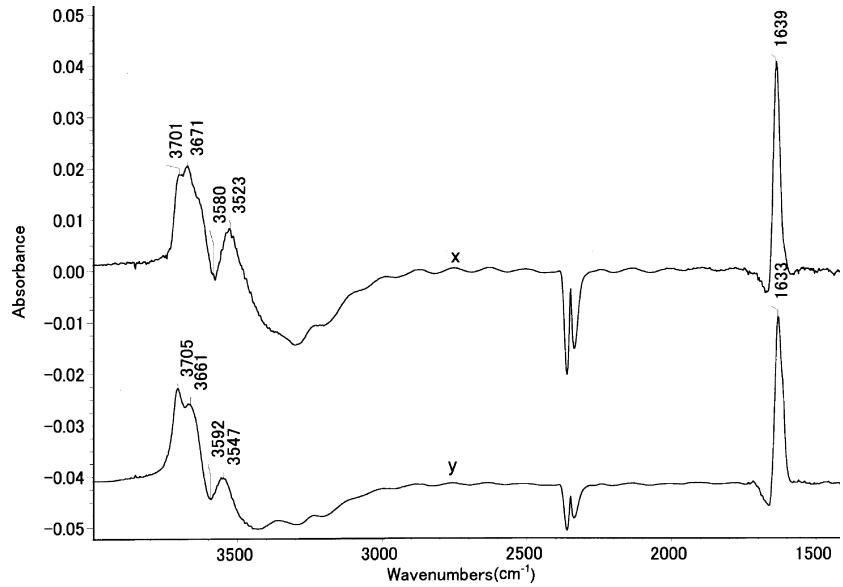

Figure 5. Double subtraction spectra of (x) SP(c−d) − SP(a−b) and (y) SP(e−f) − SP (a−b) derived from the spectra in Figure 1.

an early or middle stage of dehydration, as discussed above. The difference spectra x and y in Figure 2 contain the absorptions of the overlaying hydration shell of sH$_2$O, which appear as obscured shoulders on the high-frequency slope of the band at about 3520 cm^{-1}. However, their detailed features are seriously disturbed by the strong band around 3520 cm^{-1}. To differentiate them, we applied "double subtraction" to a series of the spectra in Figure 1. Consider two pairs of the spectra i and j, and k and l, where the notations i, j, etc. denote the measurement numbers of spectra (Table 1), and the number increases as i < j < k < l. The spectrum of j is subtracted from that of i, the difference spectrum being denoted as SP(i−j). Similarly, we obtain another difference spectrum of SP(k−l). Then, we perform a double subtraction between the two difference spectra to give [SP(k−l) − fSP(i−j)], where f is a subtraction factor.

Figure 5 shows the difference spectra of [SP(c−d) − f_1SP(a−b)] and [SP(e−f) − f_2SP(a−b)] among the spectra in Figure 1, f_1 and f_2 being appropriate subtraction factors. The spectra show two peaks at about 3700 and 3665 cm^{-1}, one valley around 3585 cm^{-1}, one peak around 3530 cm^{-1}, and a clear peak around 1630 cm^{-1}. The band around 3530 cm^{-1}, which is caused by the shift of the main band, is trivial. Appearance of the valley around 3585 cm^{-1} indicates that a hydration component with an obscured shoulder around this frequency evaporates at the very early stage of dehydration, as is observed in the difference spectrum SP(a−b) in Figure 2x. The two bands at about 3700 and 3665 cm^{-1} appear in both spectra but their relative peak heights are different between the two spectra. This means that the hydration components, which show the two bands, evaporate at different stages of dehydration. The component that evaporates at the very early stage of dehydration and shows a valley around 3590 cm^{-1} in the spectra in Figure 5 may be tentatively assigned to the hydration shell around the counterion SO_3^-, to which the water is weakly hydrogen-bonded through the H atoms. The band around 3665 cm^{-1} may be tentatively assigned to the water that is under influence of the electrostatic field of a Li^+ ion and weakly hydrogen-bonded to the first hydration or the counterion SO_3^-. The band around 3700 cm^{-1} may be assigned to a free OH of the water that is somehow coordinated through the O atom to a Li ion. These bands definitely belong to the weakly bound overlaying second hydration shell, consisting of a small number of water molecules, or sH$_2$O in [SO_3^-(Li^+·nH$_2$O)·sH$_2$O] (Isol), although it is not easy to definitely assign these bands from the spectra alone.

Here it is important to note that the separated δ(OH) band of the second hydration shell is also clear and strong in the spectra in Figure 5. This is consistent with what is observed for the first hydration shell in Figure 4. The observation consistently implies that the interaction with the electrostatic field a Li^+ ion enhances the band of a water molecule, as discussed above.

There occurs a question as to why the first hydration shell around a Na ion, and also that around a K or Rb ion, has a singlet band around 3665 cm^{-1} as in Figure 2 and Table 3, whereas the first hydration shell around a Li ion shows well-defined doublet bands of ν_3 and ν_1 vibrations. It was reported that the water in $M^+(H_2O)_n$ (n = 1 and 2) for M = Li, Na, K, and Cs shows the ν_3 and ν_1 bands of actually the same frequencies at about 3710 and 3640 cm^{-1}, respectively.[24,25] This may indicate that not only the strength of the electrostatic field of an alkali metal ion but also the counterion or SO_3^- influence on the coordinating manner of water molecules in the first hydration around an alkali metal ion in [SO_3^-(M^+·nH$_2$O)] (Isol).

Hydration Shell around a SO_3Li Group in Hydrophilic Ionic Clusters. Here we treat the hydration shell around a $SO_3^-Li^+$, which comprises a clustered ionic group, or the hydrating water in [SO_3^-(Li^+·nH$_2$O)·mH$_2$O)] (Clus) in (1), which shows the ν(OH) band at about 3520 cm^{-1}. The first hydration shell of nH$_2$O should be coordinated to a Li^+ ion, just as in the case of the isolated Li^+ ion, but the ν_1 and ν_3 bands, which do not separately appear even in the most dehydrated state, are concealed as in the spectrum h in Figure 1. This is perhaps because the first hydration shell, which is still overlaid by the second hydration shell, is not free from hydrogen bonding, which causes downward-shifting and broadened fusion of the bands. Consequently, the OH stretching band of the first hydration shell is not distinguishable from the ν(OH) band of the second hydration shell.

At this stage, we need to consider whether the second hydration shell surrounds the hydrated Li ion separately from the counterion of SO_3^- or both together. The frequency and band feature of the ν(OH) band around 3520 cm^{-1} of the

TABLE 5: Variation of the Various Infrared Spectral Characteristics of the Water in the Outer-to-Inner Divided Hydration Shells

	water	A	B	C	D	E	F	
$\Delta A/A(0)$		0.18	0.19	0.18	0.14	0.10	0.10	0.11
spectrum[a]		a − b	b − c	c − d	d − e	e − f	f − h	h
evap conditions								
flow rate (mL/min)		20	20	20	50	500	500	
time lapse (min)		6	10	32	110	273	2166	
spectral characteristics								
ν(OH) (cm^{-1})	3414	3505	3508	3510	3516	3523	3531	3530
δ(OH) (cm^{-1})	1649	1647	1643	1639	1635	1633	1631	1628
$w[\delta(OH)]$ (cm^{-1})[b]	107	62	56	50	47	43	44	
$P[\delta(OH))/P(\nu(OH))$	0.21	0.32	0.38	0.45	0.58	0.72	0.85	

[a] Differences between the spectra a, b, etc., indicated in Figure 1 or Table 1. [b] Bandwidth of the δ(OH) band.

hydration shell is independent of an alkali metal ion, as is seen from Table 3 and Figures 1 and 2. On the other hand, if we change the counterion from SO_3^- to COO^-, the main ν(OH) band shifts down from about 3520 to about 3440 cm^{-1}.[56] This implies that the second hydration shell surrounds both a *hydrated* alkali metal ion and a counterion of SO_3^- (or COO^-) together. In fact, the C−O stretching band of a COO^- group, which appears at about 1430 cm^{-1}, significantly shifts upward with the progress of dehydration. This indicates that a COO^- group is incorporated into the hydrogen bonding to the second hydration shell.[56]

A hydrated ionic group $[SO_3^-(Li^+ \cdot nH_2O) \cdot mH_2O)]$ (Clus) should be dehydrated under the flow of drying gas as follows,

$$\underset{P}{[SO_3^-(Li^+ \cdot nH_2O) \cdot mH_2O)](Clus)} \rightarrow \underset{Q}{[SO_3^-(Li^+ \cdot nH_2O) \cdot pH_2O)](Clus)} + (m-p)H_2O(\uparrow) \rightarrow$$

$$\rightarrow \underset{R}{[SO_3^-(Li^+ \cdot nH_2O)](Clus)} + pH_2O(\uparrow) \qquad (4)$$

where p is an integer ($m \geq p \geq 0$). In a series of spectra in Figure 1, the band at about 3520 cm^{-1} still remains as a main absorption in the "most dehydrated" state as in spectrum h. This implies that the innermost layer of the second hydration shell still covers the first hydration shell. This observation is clearly different from the case of the hydration shell around an isolated Li^+ ion, of which not only the second hydration shell was completely removed by evaporation but also the first hydration shell was partly evaporated at the last stage of dehydration, as discussed above. This means that *the hydration shell around a $SO_3^-Li^+$ group is far more stable in a hydrophilic environment than in a hydrophobic one.*

Evaporation of the second hydration shell should occur from its outermost layer. Each spectrum in Figure 1 shows the hydration shell at the time of a measurement in the course of its evaporation. A difference between a pair of the spectra, which were sequentially measured at t_1 and t_2 (t_1: earlier), should give the spectrum of a divided hydration shell, which remained attached at t_1 but evaporated before t_2. Thus, a series of the differences between a pair of the sequential spectra in Figure 1 or Table 1 should show how a spectrum of the divided hydration shell changes from the outer to the inner in the second hydration shell. Table 5 gives frequencies of δ(OH) and ν(OH) bands, bandwidths of δ(OH), and their relative peak heights $P(\delta(OH))/P(\nu(OH))$ in the difference spectra obtained in this manner, of the divided hydration shells. The corresponding spectral characteristics of liquid water are given for comparison in the table. The table also gives a time lapse between two relevant measurements and the relevant flow rate of drying gas for consideration. A divided shell is denoted as A, B, etc. from the outermost layer to the inner. The notation ΔA is the area intensity of the main OH stretching band in a difference spectrum, and the ratio $\Delta A/A(0)$ in the second line gives an estimated volume fraction of a divided hydration shell, with the assumption that the area intensity of the ν(OH) band over the 3700−3100 cm^{-1} region is proportional to the amount of the water contained.

According to Table 5, the spectroscopic property of a divided shell significantly changes from the outer to the inner. The outermost layer has the ν(OH) band at 3505 cm^{-1} and the δ(OH) band at 1647 cm^{-1}, and their peak-height ratio or $P[\delta(OH)]/P[\nu(OH)]$ is 0.32, as in column A. Proceeding from A to F, the ν(OH) band shifts upward by 26 cm^{-1} to 3531 cm^{-1} and the δ(OH) band, on the contrary, shifts downward by 16 cm^{-1} to 1631 cm^{-1} and the peak-height ratio increases to 0.85. The innermost layer, which does not evaporate even after prolonged dehydration, shows the ν(OH) band at 3530 cm^{-1} and the δ(OH) band at 1628 cm^{-1}.

Here let us focus on the above-mentioned *noteworthy* frequency shift of ν(OH) and δ(OH) bands, which depends on the depth from the outermost hydration layer. The observed shift direction of the bands means that the hydrogen bond becomes weaker from the outer to the inner in the second hydration shell, since it is against the experimental rule that stronger hydrogen bond causes the ν(OH) to shift downward and the δ(OH) band to shift upward.[29,31,52] On the other hand, Tables 1 and 5 clearly indicate that the inner hydration shell is more strongly attracted in the membrane. The phenomena are reasonably interpreted as follows. The electrostatic field of a Li^+ ion, which is stronger at a position nearer to the ion, should more strongly interact with the polar molecule of water in the inner second hydration shell. That stronger electrostatic interaction should induce a more ordered molecular arrangement of the water in the inner second hydration shell,[57] which is less favorable for intermolecular hydrogen-bonding. This is consistent with the theoretical study that the electrostatic interaction of water with a Li^+ ion makes a considerable contribution to the hydration energy of the second hydration shell,[10] and with the observation that the frequencies of the ν(OH) and δ(OH) bands of the hydration shell around the $SO_3^-Na^+$ group depend little on the progress of dehydration as shown in Figure 3. This means that the electrostatic field of a Na ion, which is significantly weaker than that of a Li^+ ion, is not so strong as to induce the molecular ordering that is less favorable for intermolecular hydrogen bonds in the inner second hydration shell. The difference was also observed for the COOLi and COONa salt membranes.[56]

Conclusion

It is well-known that the hydration shell around an alkali ion in aqueous solution consists of the first hydration shell and the

overlaying second hydration shell.[5,7,58] The structure of the first hydration shell is well understood experimentally and theoretically,[58] but experimental information about the structure and property of the second hydration shell is poor.[58] In the present study we investigated the change, which followed prolonged dehydration, in the infrared spectrum of the hydration shell around the electrolytic $SO_3^-M^+$ group in a Nafion membrane. We found that the membrane contains a minor component of the $SO_3^-M^+$ groups, which are *individually isolated* in a hydrophobic matrix, in addition to the main component of the clustered groups. We denote the isolated and clustered groups as I and II, respectively, hereafter for convenience. From the spectral observations of the hydration shells around I and II, we may propose a model of the hydration shell around a $SO_3^-Li^+$ group, as follows.

We resolved the infrared spectrum of the first hydration shell, which clearly shows all the ν_1, ν_2, and ν_3 fundamental bands, from the hydration shell around I. On the other hand, we found from the hydration shell around II that the infrared spectroscopic properties of the second hydration shell significantly change from the outer to the inner (Table 5). That is, the shift tendency observed of the ν(OH) and δ(OH) bands consistently implies that *the strong electric field of a Li ion influences the molecular arrangement so as to be less favorable for intermolecular hydrogen-bonding in the inner second hydration shell*. The ratio $A/A(0)$ in Table 1 gives a rough estimation of the thickness of the second hydration shell outside the first hydration shell. The table indicates that two-thirds of the whole hydration shell evaporates under moderate dehydration conditions, and two-thirds of the remaining part evaporates at the last stage of the prolonged dehydration under the highest flow rate of drying gas, but the other one-third does not evaporate even after the full dehydration. If we assume that the spectrum h in Figure 1, which still remains after the full dehydration, is of the "core shell" around $SO_3^-Li^+$, which consists of "the first hydration shell and the innermost mono-molecular layer of the second hydration shell", the thickness of the whole second hydration in the fully hydrated state at atmospheric humidity is estimated to be two or three molecular layers outside the core shell.

The ν_2 band of the first hydration shell around a Li ion is stronger than the ν_3 or ν_1 fundamental, although the opposite is true for the water isolated in a weakly interacting medium. Intermolecular hydrogen bonds are increasingly broken in the inner second hydration shell under the stronger electrostatic field of a Li^+ ion, as discussed above. This is the first clear spectroscopic evidence, to our knowledge, for the effect that the electrostatic field of a Li^+ ion exerts on its hydration shell or the effect of electrostriction.[12,59]

References and Notes

(1) Licheri, G.; Piccaluga, G.; Pinna, G. *J. Appl. Crystallogr.* **1973**, *6*, 392–395.

(2) Narten, A. H.; Vaslow, F.; Levy, H. A. *J. Chem. Phys.* **1973**, *58*, 5017–5023.

(3) Ohtomo, N.; Arakawa, K. *Bull. Chem. Soc. Jpn.* **1979**, *52*, 2755–2759.

(4) Newsome, J. R.; Neilson, G. W.; Enderby, J. E. *J. Phys. C: Solid St. Phys.* **1980**, *13*, L923–6.

(5) Radnai, T.; Palinkas, G.; Szasz, G. I.; Heizinger, K. *Z. Naturforsch.* **1981**, *A36*, 1076–1082.

(6) Enderby, J. E.; Cummings, S.; Herdman, G. J.; Neilson, G. W.; Salmon, P. S.; Skipper, N. *J. Phys. Chem.* **1987**, *91*, 5851–5858.

(7) Howell, I.; Neilson, G. W. *J. Phys.: Condens. Matter.* **1996**, *8*, 4455–4463.

(8) Pye, C. C.; Rudolph, W.; Poirier, R. A. *J. Phys. Chem.* **1996**, *100*, 601–605.

(9) Tongraar, A.; Liedl, K. R.; Rode, B. M. *Chem. Phys. Lett.* **1998**, *286*, 56–64.

(10) Hashimoto, K.; Kamimoto, T. *J. Am. Chem. Soc.* **1998**, *120*, 3560–3570.

(11) Hermansson, L; Wojcik, M. *J. Phys. Chem. B* **1998**, *102*, 6089–6097.

(12) Babu, C. S.; Lim, C. *J. Phys. Chem. B* **1999**, *103*, 7958–7968.

(13) Pye, C. C. *Int. J. Quantum Chem.* **2000**, *76*, 62–76.

(14) Rempe, S. B.; Pratt, L. R.; Hummer, G.; Kress, J. D.; Martin, R. L.; Redondo, A. *J. Am. Chem. Soc.* **2000**, *122*, 966–967.

(15) Yamaji, K.; Makita, Y.; Watanabe, H.; Sonoda, A.; Kano, H.; Hirotsu, T.; Ooi, K. *J. Phys. Chem., A* **2001**, *105*, 602–613.

(16) Topol, I. A.; Tawa, G. J.; Burt, S. K. *J. Chem. Phys.* **1999**, *111*, 10998–11014.

(17) Egorov, A. V.; Momolkin, A. V.; Chizhik, V. I.; Yushmanov, P. V.; Lyubartsev, A. P.; Laaksonen, A. *J. Phys. Chem. B* **2003**, *107*, 3234–3242.

(18) Spangberg, D.; Rey, R.; Hynes, J. T.; Hermansson, K. *J. Phys. Chem. B* **2003**, *107*, 4470–4477.

(19) Lee, H. M.; Tarakeshwar, P.; Park, J.; Kolaski, M. R.; Yoon, Y. J.; Yi, H.-B.; Kim, W. Y.; Kim, K. S. *J. Phys. Chem. A* **2004**, *108*, 2949–2958.

(20) Oehrn, A.; Karlstroem, G. *J. Phys. Chem. B* **2004**, *108*, 8452–8459.

(21) Watanabe, H.; Ooi, K. *J. Phys. Chem. A* **2005**, *109*, 9844–9855.

(22) Li, X.; Yang, Z.-Z. *J. Phys. Chem. A* **2005**, *109*, 4102–4111.

(23) Loeffler, H. H.; Inada, Y.; Funahashi, S. *J. Phys. Chem. B* **2006**, *110*, 5690–5696.

(24) Miller, D. J.; Lisy, J. M. *J. Am. Chem. Soc.* **2008**, *130*, 15381–15392.

(25) Miller, D. J.; Lisy, J. M. *J. Am. Chem. Soc.* **2008**, *130*, 15393–15404.

(26) Rao, J. S.; Dinadayalane, T. C.; Leszczynski, J.; Sastry, G. N. *J. Phys. Chem. A* **2008**, *112*, 12944–12953.

(27) Petit, L.; Vuilleumier, R.; Maldivi, P.; Adamo, C. *J. Chem. Theory Comput.* **2008**, *4*, 1040–1048.

(28) Benjamin, I. *J. Phys. Chem. B* **2008**, *112*, 15801–15806.

(29) Jeffrey, G. A. *An Introduction to Hydrogen Bonding*; Oxford University Press: Oxford, U.K., 1997; pp 213−226.

(30) Bellamy, L. J. *The Infrared Spectra of Complex Molecules, Vol. 2: Advances in Infrared Group Frequencies*, 2nd ed.; Chapman and Hall: London, 1980; Chapter 8.

(31) Glew, D. N.; Rath, N. S. *Can. J. Chem.* **1971**, *49*, 837–856.

(32) Rudolf, W.; Brooker, M. H.; Pye, C. C *J. Phys. Chem.* **1995**, *99*, 3793–3797.

(33) Max, J. -J.; Chapados, C. *J. Chem. Phys.* **2001**, *115*, 2664–2675.

(34) Smiechowski, M.; Gojlo, E.; Stangret, J. *J. Phys. Chem. B* **2004**, *108*, 15938–15943.

(35) Wachter, W.; Fernandez, S.; Buchner, R.; Hefter, G. *J. Phys. Chem. B* **2007**, *111*, 9010–9017.

(36) Park, S.; Moilanen, D. E.; Fayer, D. *J. Phys. Chem. B* **2008**, *112*, 5279–5290.

(37) Perera, P. N.; Browder, B.; Ben-Amotz, D. *J. Phys. Chem. B* **2009**, *113*, 1805–1809.

(38) Smith, J. D.; Saykally, R. J.; Geissler, P. L. *J. Am. Chem. Soc.* **2007**, *129*, 13847–13856.

(39) Robertson, M. A. F.; Yeager, H. L. Structure and properties of perfluorinated ionomers. In *Ionomers: Synthesis, Structure, Properties and Applications*; Tant, M. R., Mauritz, K. A., Wilkes, G. L., Eds.; Chapman & Hall: New York, 1997; pp 290−330.

(40) Fujimura, M.; Hashimoto, T.; Kawai, H. *Macromolecules* **1981**, *14*, 1309–1315.

(41) Fujimura, M.; Hashimoto, T.; Kawai, H. *Macromolecules* **1982**, *15*, 136–144.

(42) Petersen, M. K.; Voth, G. A. *J. Phys. Chem. B* **2006**, *110*, 18594–18600.

(43) Freger, V. *J. Phys. Chem. B* **2009**, *113*, 24–36.

(44) Hofmann, D. W. M; Kuleshova, L.; D'Aguanno, B.; Noto, V. D.; Negro, E.; Conti, F.; Vittadello, M. *J. Phys. Chem. B* **2009**, *113*, 632–639.

(45) Spry, D. B.; Fayer, M. D. *J. Phys. Chem. B* **2009**, *113*, 10210–10221.

(46) Falk, M. *Can. J. Chem.* **1980**, *58*, 1495–1501.

(47) Quezado, S.; Kwak, J. C. T.; Falk, M. *Can. J. Chem.* **1984**, *62*, 958–966.

(48) Iwamoto, R.; Oguro, K.; Sato, M.; Iseki, Y. *J. Phys. Chem. B* **2002**, *106*, 6973–6979.

(49) The shape of the band around 2350 cm^{-1} appears to change depending on the time period of dehydration. This is because the absorption of CO_2 around 2300 cm^{-1} is not just balanced between a spectrum measured at a time and a background spectrum, which was measured several times through the whole measurement. Around the frequency, an absorption due to the polymer of the membrane additionally appears, which is assigned to the first combination band of the C−F stretching absorptions at 1204 and 1150 cm^{-1}.

(50) Iwamoto, R.; Matsuda, T.; Amiya, S.; Yamamoto, T. *J. Polym. Sci., Part B: Polym. Phys* **2006**, *44*, 2425–2437.
(51) Iwamoto, R.; Kusanagi, H. *J. Phys. Chem. A* **2009**, *113*, 5310–5316.
(52) Iwamoto, R.; Matsuda, T.; Kusanagi, H. *Spectrochim. Acta, Part A* **2005**, *62*, 97–104.
(53) Iwamoto, R.; Matsuda, T. *Spectrochim. Acta, Part A* **2005**, *62*, 1016–1022.
(54) Iwamoto, R. Unpublished work.
(55) Kusanagi, H.; Yukawa, S. *Polymer* **1994**, *35*, 5637–5640.
(56) Iwamoto, R. Unpublished work.
(57) Hribar, B.; Southhall, N. T.; Vlachy, V.; Dill, K. A. *J. Am. Chem. Soc.* **2002**, *124*, 12302–12311.
(58) Ohtaki, H.; Radnai, T. *Chem. Rev.* **1993**, *93*, 1157–1204.
(59) Burgess, J. *Ions in Solution*, 2nd ed.; Horwood Publishing: Chichester, U.K., 1999; pp 57−58.

JP906934U